

NiO/ZnO light emitting diodes by solution-based growth

Y. Y. Xi,¹ Y. F. Hsu,¹ A. B. Djurišić,^{1,a)} A. M. C. Ng,¹ W. K. Chan,² H. L. Tam,³ and K. W. Cheah³

¹Department of Physics, The University of Hong Kong, Pokfulam Road, Hong Kong

²Department of Chemistry, The University of Hong Kong, Pokfulam Road, Hong Kong

³Department of Physics, Hong Kong Baptist University, Kowloon Tong, Hong Kong

(Received 9 January 2008; accepted 26 February 2008; published online 17 March 2008)

Heterojunction NiO/ZnO light emitting diodes have been fabricated using low temperature solution-based growth methods. While negligible light emission has been obtained for the as-grown NiO film, devices with annealed NiO film exhibit room-temperature electroluminescence (EL), which was attributed to the detrimental effects of nickel oxide hydroxide in as-grown NiO layers. The device performance can be further modified by insertion of the organic layers between NiO and ZnO and the EL spectra exhibited dependence on the bias voltage. For higher bias voltages, strong UV-violet emission peak can be obtained in spite of the dominance of defect emission in the photoluminescence spectra. © 2008 American Institute of Physics. [DOI: 10.1063/1.2898505]

Both homojunction¹⁻³ and heterojunction^{1,4-7} light emitting diodes (LEDs) based on ZnO have been reported to date. Realization of homojunction devices is difficult due to problems in achieving stable and reliable *p*-type doping¹ and achieved emission is typically weak,^{2,3} unless barrier layers such as (Mg,Zn)O are used.³ For heterostructure devices, a variety of *p*-type semiconductors (GaN,^{1,4} Si,^{5,6} SrCu₂O₂,⁷ SiC,¹ Cu₂O,¹ etc.) could be used, although electroluminescence (EL) under forward bias has been observed only in some of these devices, and in many cases, observed EL was weak.¹

Many of the reports of UV EL in ZnO are based on the epitaxial ZnO layers,⁷ which require lattice-matched substrates, deposition of buffer layers, and the use of relatively high temperature and high cost growth methods. In this work, we used low temperature, low cost solution-based growth methods for both *p*-type NiO film and *n*-type ZnO nanorods. Although NiO is a transparent *p*-type semiconductor and NiO/ZnO heterojunctions for photodetector applications exhibited clear rectifying properties,^{8,9} no LEDs with *p*-NiO/*n*-ZnO heterojunctions have been reported. Also, while NiO can also be fabricated by a simple electrochemical deposition on a conductive substrate,¹⁰ this method is rarely used for fabrication of devices. However, under optimized deposition conditions developed here, films with densely packed small grains can be obtained instead of a flaky nanowall morphology that is commonly obtained for electrodeposited¹⁰ or hydrothermally grown NiO. As for ZnO, although hydrothermally grown ZnO nanorods¹¹⁻¹³ typically have inferior optical properties compared to the vapor deposited ones,¹⁴ we show here that UV EL can be obtained in spite of weak UV emission in photoluminescence (PL) spectra.

NiO film was fabricated using a two electrode system at a deposition temperature of 50 °C. An indium tin oxide (ITO)/glass and a Pt wire were used as the cathode and anode, respectively. The electrolyte was an aqueous solution containing 0.2M nickel nitrate hexahydrate and 0.2M hexamethylenetetramine (HMT) (99+%). The voltage during

deposition was 2.2 V and the deposition time was 1 min. Then, the seed layer [electrodeposited (ED) seed] for ZnO nanorod growth was prepared using electrodeposition from ethanol/water solution, which contained 0.04M zinc nitrate hydrate (99.999%) and 0.015M HMT and using zinc foil (99.99%) as the counterelectrode. The voltage was set to be 0.8 V and the reaction time was 1 min. The sample was then dried in an oven. Following the deposition of seed layers, ZnO nanorods were grown by a hydrothermal method¹¹⁻¹³ in an aqueous solution containing polyethyleneimine, zinc nitrate hydrate, and HMT for 2.5 h.¹²

The morphology of the rods was studied by scanning electron microscopy (SEM), while the optical properties were studied by PL spectroscopy using HeCd laser (325 nm) as the excitation source. The *I*-*V* relationship of the devices was measured by Keithley 2400 sourcemeter and the EL spectra were collected using a monochromator with Peltier-cooled photomultiplier detector. The following device structures were investigated: device I: ITO/NiO (200 nm)/ED seed/ZnO nanorods (300 nm)+spin on glass (SOG) (Intermediate Coating IC1-200, polysiloxane-based dielectric material)/Al (100 nm), device II: ITO/NiO/4,4',4''-Tris (*N*-3-methylphenyl-*N*-phenyl-amino)-triphenylamine (MTDATA) (H. W. Sands) (30 nm)/ED seed/ZnO nanorods +SOG/Al (100 nm), and device III: ITO/NiO/poly(4-vinylpyridine) (PVP) (Aldrich, Mw 60 000) /ED seed/ZnO nanorods+SOG/Al (100 nm). MTDATA and Al films were prepared by thermal evaporation in high vacuum (10⁻⁴ Pa), while PVP was deposited by simple adsorption from chloroform solution (10 mg PVP in 4 ml chloroform). After 4 h in the solution, the samples were rinsed with chloroform to remove residue and dried. The function of a SOG layer in nanorod devices is to prevent a direct contact between the top contact and the *p*-type layer/bottom electrode which could lead to short circuit.⁵ The function of the MTDATA was to reduce the barrier for the hole injection into ZnO since the highest occupied molecular orbital (HOMO) level of this material is between the valence band level of NiO (4.9 eV) (Ref. 10) and ZnO (7.6 eV).¹⁵ HOMO level of MTDATA is ~5.1 eV.¹⁶ Unlike MTDATA which is a hole transporting material, PVP is an insulating polymer. Thin organic

^{a)}Electronic mail: dalek@hkusua.hku.hk.

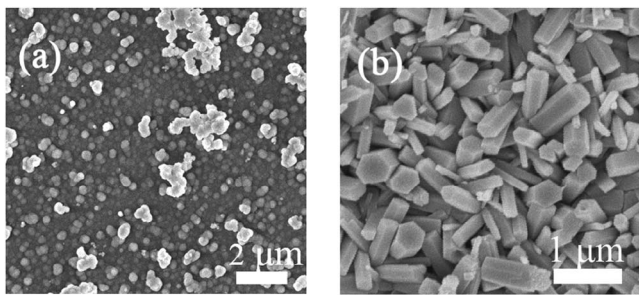


FIG. 1. SEM images of (a) NiO film (b) ZnO nanorods on NiO.

layers can cause a shift of the energy levels due to surface dipoles, although the amount and the direction of the shift is strongly material dependent.¹⁷ We have used PVP thin layer since it can be deposited using a simple adsorption from solution.

Figure 1 shows the SEM images of a NiO film and ZnO nanorods grown on the NiO film. NiO film consists of compact, closely packed grains [Fig. 1(a)]. Unlike ZnO nanorods grown from zinc acetate derived seed,^{11–13} ZnO nanorods grown on ED seed layer on ED NiO [Fig. 1(b)] have random orientation on the substrate. The lack of size and orientation uniformity is likely due to the properties of the ED seed layer since ED seed yields rods which are not well oriented on ITO substrate. This is also confirmed by x-ray diffraction (XRD) patterns, as shown in Fig. 2. In spite of the random orientations of ZnO nanorods with respect to the substrate, NiO/ZnO heterojunctions exhibit good rectifying properties, as shown in Fig. 3(a). However, very weak light emission (barely detectable by naked eye, EL spectrum too noisy to be reliably measured) was observed from these devices. On the other hand, EL could be obtained if NiO layer was annealed at 200 °C [for 30 min in Ar gas flow of 0.1 lpm (lpm denotes liters per minute)]. While the morphology of the films exhibits no significant difference before and after annealing, in XRD patterns obvious differences can be observed, as shown in Fig. 2. In as-grown films, peaks corresponding to nickel oxide hydroxide are obtained, while peaks corresponding to NiO are weak. After annealing at 200 °C, only

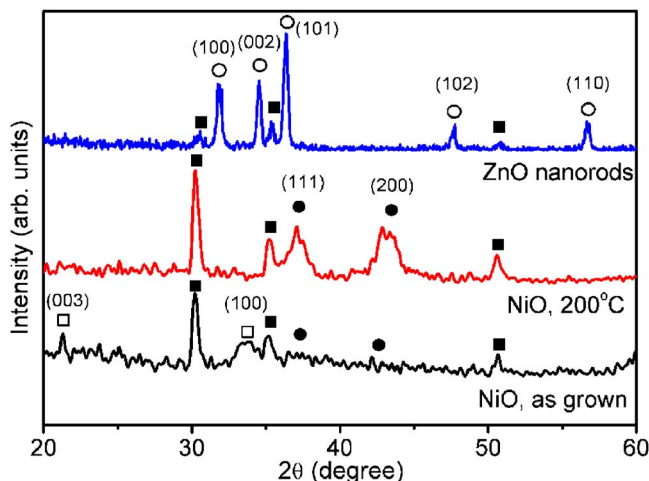


FIG. 2. (Color online) XRD spectrum of NiO (before and after annealing) and ZnO on ITO substrates. Black squares denote ITO substrate, black circles denote peaks corresponding to NiO, open circles denote peaks corresponding to ZnO, while open squares denote peaks corresponding to nickel oxide hydroxide.

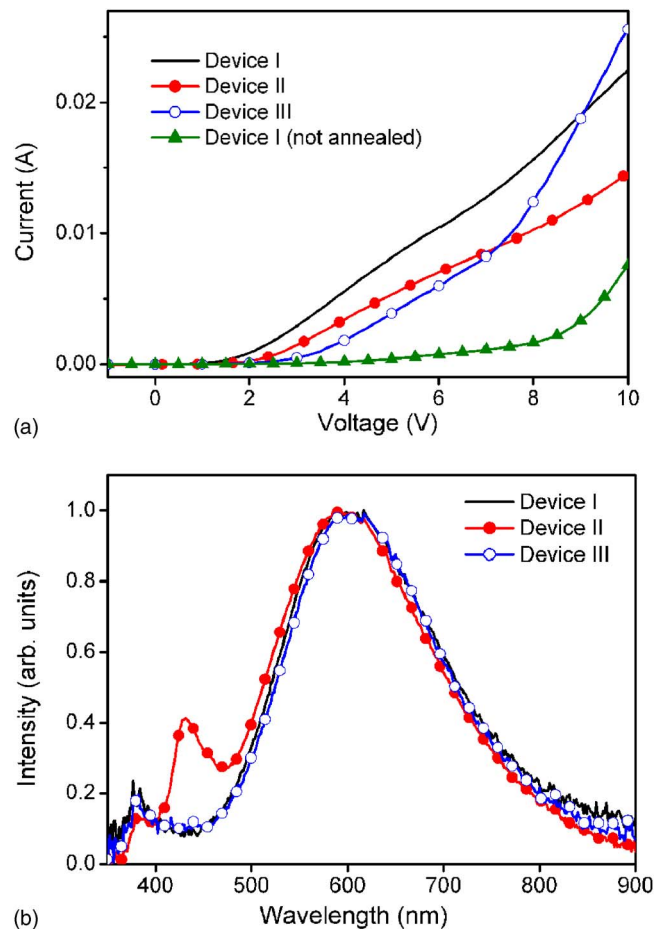


FIG. 3. (Color online) (a) I - V curves and (b) PL of different heterojunction devices.

NiO peaks can be found. Thus, the presence of nickel oxide hydroxide in as-grown NiO layers leads to the quenching of the light emission.

I - V curves and the PL spectra of devices I–III are shown in Fig. 3. The differences among the devices are due to their structures (presence of additional layers in devices II and III). It can be observed that all the devices exhibit diodelike behavior, including device I without annealing for NiO layer, although this device does not have good light-emitting properties. All the PL spectra are dominated by the yellow-orange defect emission band, which can be attributed to the presence of OH groups on the surface and defect complexes in the nanorods.¹³ The blue emission peak in device II is due to the emission from MTDATA layer.

Significant differences can be observed between the PL spectra [Fig. 3(b)] and the EL spectra [Fig. 4(a)]. The differences between the PL and EL spectra are likely due to differences in carrier concentration profiles in the devices in the case of optical and electrical excitation, which can result in differences in position of the recombination region and/or dominant recombination mechanism. For devices I and III, UV-violet emission peak is considerably more prominent than in the EL spectrum, while for device II, very broad visible emission was observed, which likely partly originates from MTDATA and partly from ZnO. In all devices, EL emission at longer wavelengths is increased compared to the PL spectra. Red emission band (~ 650 nm) was reported in EL spectra of ZnO homojunction LEDs¹⁸ and it was absent in the PL spectra. From the positions of the energy levels of

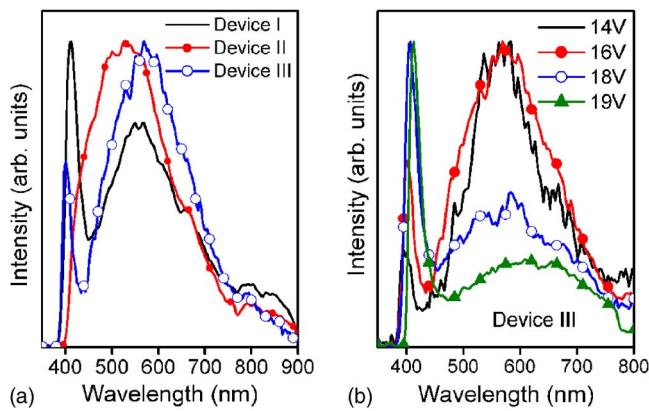


FIG. 4. (Color online) (a) EL spectra of devices I–III under bias voltage of 16 V. (b) EL spectra of device III at different bias voltages.

the materials used,^{10,15,16} direct formation of the electropoles in the range of 600–800 nm can be excluded so that defect energy levels in ZnO likely contribute to this emission.

For both devices II (not shown) and III, we observed the increase of UV-violet emission peak with increased bias voltage. For device II, although the emission spectrum at bias voltage $V_b=16$ V exhibits only a broad visible emission, for $V_b=18$ V the spectrum is dominated by a UV-violet peak which is about twice more intense than the broad visible emission. For device III, as shown in Fig. 4(b), steady increase of the UV-to-visible emission ratio is obtained for increased bias voltage, in agreement with some of the reported behavior of ZnO LEDs.⁵ In homojunction ZnO LEDs, increase in the intensity and blueshift of the defect emission has been observed with the increase of the injection currents.³ Similar increase of the visible emission with increased injection current but without the blueshift was also observed in *n*-ZnO/*p*-Si heterojunction LEDs.⁶ On the other hand, increase of the bias voltage in *p*-GaN/*n*-ZnO nanorod LEDs resulted in the increase of the blue emission and appearance of UV peak (from *p*-GaN) at higher bias voltages.⁴ However, in previous reports, lower UV-to-visible ratio was obtained in EL compared to PL spectra.^{4,5} Since dominant UV-violet emission is obtained in the EL spectra in spite of the negligible band edge emission in PL spectra and the opposite behavior reported in the literature,^{4,5} we can conclude that PL spectra do not represent a good indicator of the device performance of ZnO based LEDs. Changes in the emission spectra with bias voltage have also been observed in LEDs based on CdTe nanoparticles, where emission shifts have been attributed to the surface states and trap centers, as well as quantum confined Stark effect.¹⁹ While quantum confined Stark effect is not an issue for large ZnO nanorods, the influence of traps and surface states on the emission spectra requires further study.

Concerning the turn-on voltage, light emission has been observed by naked eye at bias of 11 V for device I, 9 V for device II, and 8 V for device III. The effect of the insertion of an organic layer on the turn-on voltage is possibly due to dipole formation at the interfaces, which affects the alignment of the energy levels at the interface.¹⁷ To optimize the device structure, it is necessary to study the actual energy level alignment at the interfaces of the devices rather than

assume the reported energy levels from the literature. Nevertheless, insertion of a PVP layer resulted in lower turn-on voltage and improved stability of the devices at higher bias voltages. However, the efficiency needs further improvement (maximum emission power $0.14 \mu\text{W}/\text{cm}^2$ at 23 V bias). The devices exhibit little sensitivity to storage in atmosphere (light emission is still obtained after more than two months storage in air without any encapsulation), while under continuous bias at 15 V in air, the emission intensity drops by 50% within the first hour. It is expected that further improvements in the performance could be achieved for suitably chosen materials.

To summarize, light emitting diodes have been fabricated using a low temperature solution-based method both for *p*-type NiO film and *n*-type ZnO nanorods. The growth technique is fully compatible with deposition of organic interlayers which can be used to modify the energy band alignment or the emission spectra of the devices. Prominent UV-violet emission peak was observed at room temperature.

This work was supported by the Research Grants Council of The Hong Kong Special Administrative Region, China (Project Nos. HKU 7021/03P, HKU 7019/04P, and 7010/05P). Financial support from the Strategic Research Theme, University Development Fund, Seed Funding Grant and Outstanding Young Researcher Award (administrated by The University of Hong Kong), and Hung Hing Ying Physical Sciences research Fund are also acknowledged.

¹Ü. Özgür, Ya. I. Alivov, C. Lin, A. Teke, M. A. Reshchikov, S. Dogan, V. Avrutin, S.-J. Cho, and H. Morkoc, *J. Appl. Phys.* **98**, 041301 (2005).

²A. Tsukazaki, A. Ohtomo, T. Onuma, M. Ohtani, T. Makino, M. Sumiya, K. Ohani, S. F. Chichibu, S. Fuke, Y. Segawa, H. Ohno, H. Koinuma, and M. Kawasaki, *Nat. Mater.* **4**, 42 (2005).

³J.-H. Lim, C.-K. Kang, I.-K. Park, D.-K. Hwang, and S.-J. Park, *Adv. Mater. (Weinheim, Ger.)* **18**, 2720 (2006).

⁴W. I. Park and G.-C. Yi, *Adv. Mater. (Weinheim, Ger.)* **16**, 87 (2004).

⁵H. Sun, Q.-F. Zhang, and J.-L. Wu, *Nanotechnology* **17**, 2271 (2006).

⁶J. D. Ye, S. L. Gu, S. M. Zhu, W. Liu, S. M. Liu, R. Zhang, Y. Shi, and Y. D. Zheng, *Appl. Phys. Lett.* **88**, 182112 (2006).

⁷H. Ohta, K. Kawamura, M. Orita, M. Hirano, N. Sarukura, and H. Hosono, *Appl. Phys. Lett.* **77**, 475 (2000).

⁸H. Ohta, M. Hirano, K. Nakahara, H. Maruta, T. Tanabe, M. Kamiya, T. Kamiya, and H. Hosono, *Appl. Phys. Lett.* **83**, 1029 (2003).

⁹Y. Vygarenko, K. Wang, and A. Nathan, *Appl. Phys. Lett.* **89**, 172105 (2006).

¹⁰K. Nakaoka, J. Ueyama, and K. Ogura, *J. Electroanal. Chem.* **571**, 93 (2004).

¹¹M. Law, L. E. Greene, J. C. Johnson, R. Saykally, and P. Yang, *Nat. Mater.* **4**, 455 (2005).

¹²L. E. Greene, M. Law, D. H. Tan, M. Montano, J. Goldberger, G. Somorjai, and P. Yang, *Nano Lett.* **5**, 1231 (2005).

¹³K. H. Tam, C. K. Cheung, Y. H. Leung, A. B. Djurišić, C. C. Ling, C. D. Belling, S. Fung, W. M. Kwok, W. K. Chan, D. L. Phillips, L. Ding, and W. K. Ge, *J. Phys. Chem. B* **110**, 20865 (2006).

¹⁴A. B. Djurišić and Y. H. Leung, *Small* **2**, 944 (2006).

¹⁵R. A. Powell, W. E. Spicer, and J. C. McMenamin, *Phys. Rev. B* **6**, 3056 (1972).

¹⁶K. Itomo, H. Ogawa, and Y. Shirota, *Appl. Phys. Lett.* **72**, 636 (1998).

¹⁷H. Ishii, H. Oji, E. Ito, N. Hayashi, D. Yoshimura, and K. Seki, *J. Lumin.* **87-89**, 61 (2000).

¹⁸Z. P. Wei, Y. M. Lu, D. Z. Shen, Z. Z. Zhang, B. Yao, B. H. Li, J. Y. Zhang, D. X. Zhao, X. W. Fan, and Z. K. Tang, *Appl. Phys. Lett.* **90**, 042113 (2007).

¹⁹W. Chen, D. Grouquist, and J. Roark, *J. Nanosci. Nanotechnol.* **2**, 1 (2002).